**Atmospheric
Chemistry
and Physics**

CO$_2$, δO$_2$/N$_2$ and APO: observations from the Lutjewad, Mace Head and F3 platform flask sampling network

I. T. van der Laan-Luijkx[1,**], **U. Karstens**[2], **J. Steinbach**[2], **C. Gerbig**[2], **C. Sirignano**[1,*], **R. E. M. Neubert**[1],
S. van der Laan[1,**], **and H. A. J. Meijer**[1]

[1]Centre for Isotope Research (CIO), University of Groningen, Groningen, the Netherlands
[2]Max Planck Institute for Biogeochemistry, Jena, Germany
[*]currently at: CIRCE, Department of Environmental Sciences, Second University of Napels, Caserta, Italy
[**]currently at: Climate and Environmental Physics, Physics Institute, University of Bern, Bern, Switzerland

Abstract. We report results from our atmospheric flask sampling network for three European sites: Lutjewad in the Netherlands, Mace Head in Ireland and the North Sea F3 platform. The air samples from these stations are analyzed for their CO$_2$ and O$_2$ concentrations. In this paper we present the CO$_2$ and O$_2$ data series from these sites between 1998 and 2009, as well as the atmospheric potential oxygen (APO). The seasonal pattern and long term trends agree to a large extent between our three measurement locations. We however find a changing gradient between Mace Head and Lutjewad, both for CO$_2$ and O$_2$. To explain the potential contribution of fossil fuel emissions to this changing gradient we use an atmospheric transport model in combination with CO$_2$ emission data and information on the fossil fuel mix per region. Using the APO trend from Mace Head we obtain an estimate for the global oceanic CO$_2$ uptake of 1.8 ± 0.8 PgC/year.

1 Introduction

Climate change and its causes and effects have been a subject of intensive research during the past decades. Climate change is primarily induced by changes in the atmosphere's composition, specifically the rapid increase in the concentrations of the greenhouse gases CO$_2$, CH$_4$, N$_2$O and halocarbons (e.g. IPCC, 2007). Anthropogenic carbon dioxide is the most significant contributor to climate change, therefore a thorough comprehension of the global carbon cycle and the main processes involving CO$_2$ is essential.

Combined atmospheric O$_2$ and CO$_2$ measurements yield valuable information about carbon cycle processes, that cannot be acquired from measurements of CO$_2$ concentrations alone (e.g. Bender et al., 1996; Keeling and Garcia, 2002; Keeling et al., 1993; Keeling and Shertz, 1992; Machta, 1980; Manning and Keeling, 2006). Most processes show an inverse relationship between O$_2$ and CO$_2$ (e.g. fossil fuel combustion, photosynthesis and respiration), but in the exchange between the ocean and the atmosphere O$_2$ and CO$_2$ are uncoupled. Marine CO$_2$ uptake leads to a chemical reaction with the ocean water, leading to a CO$_2$ buffer effect. The uptake of O$_2$ does not have this effect, as O$_2$ merely dissolves in water and this is independent of the CO$_2$ uptake process. Combined measurements of atmospheric O$_2$ and CO$_2$ can therefore be used to partition land and ocean CO$_2$ uptake (e.g. Battle et al., 2000; Bender et al., 2005; Keeling and Shertz, 1992; Langenfelds et al., 1999; Manning and Keeling, 2006).

Since changes in the atmospheric O$_2$ concentration are in most processes directly related to changes in the CO$_2$ concentrations, they occur in the same order of magnitude. However, the changes in O$_2$ are harder to detect as they are to be measured against a much larger background. High precision measurements of atmospheric O$_2$ have begun in 1988 when R. F. Keeling developed an instrument based on interferometry (Keeling, 1988a, b). Since then other methods have been developed to enable atmospheric O$_2$ measurements at the required precision of 1:10^6 (WMO, 2009). Current techniques include mass-spectrometry (Bender et al., 1994), paramagnetic analyzers (Manning et al., 1999), vacuum ultraviolet absorption (Stephens, 1999; Stephens et al., 2003), gas chromatography (Tohjima, 2000) and fuel cells (Patecki and Manning, 2007; Stephens et al., 2007; Thompson et al., 2007). Each of these techniques has its specific

Correspondence to: I. T. van der Laan-Luijkx
(i.t.luijkx@rug.nl)

advantages and disadvantages, not only related to the O_2 sensor obtaining the required precision, but also to the possibility to run the instrument automatically, remotely or in harsh conditions, e.g. on moving platforms, like ships or aircrafts.

The first systematic measurements of atmospheric O_2 were performed by Keeling and Shertz (1992) at three measurement sites from north to south: Alert (82.5° N, 62.3° W), La Jolla (32.9° N, 117.3° W) and Cape Grim (40.7° S, 114.7° E), showing seasonal patterns and interannual O_2 variations in different environments on both hemispheres. Since then the amount of sampling sites has increased during the past two decades from these three to over 20, including both stations where flasks are sampled as well as those with continuous monitoring of atmospheric O_2 (e.g. Battle et al., 2006; Kozlova et al., 2008; Manning and Keeling, 2006; Popa et al., 2009; Thompson et al., 2009; Tohjima et al., 2008). In this paper we will contribute new observations from the flask sampling stations Lutjewad in the Netherlands (2005–2009), Mace Head in Ireland (2005–2009 and winter 1998/1999) and the F3 North Sea platform (2006–2009), extending earlier work presented by Sirignano et al. (2010). For the F3 North Sea platform we also combine the flask samples with the first continuous onsite measurements (van der Laan-Luijkx et al., 2010).

In this paper we first describe the measurement stations (Sect. 2), and continue with the flask sampling strategies and measurement methods (Sect. 3.1). Sections 3.2 and 3.3 give background information on the O_2 calculations and Atmospheric Potential Oxygen (APO). The regional model REMO, which we use to investigate the influence of regional differences in the fossil fuel oxidative ratio is described in Sect. 3.4. In Sect. 4 we present our observations of CO_2, O_2 and APO at the three stations and discuss their variability, trends and gradients. Finally, we give an estimate for global marine CO_2 uptake based on the observations from Mace Head.

2 Descriptions of the measurement stations

Figure 1 shows the locations of our three monitoring stations. The Lutjewad atmospheric monitoring station is situated on the northern coast of the Netherlands, at 53°24′ N, 6°21′ E, 1 m a.s.l, alongside the Wadden Sea. The station comprises a 60 m high tower as well as a laboratory with an automated flask sampler and instruments for in-situ measurements. Several atmospheric gases and other characteristics are measured at Lutjewad including continuous measurements of CO_2, CH_4, CO, N_2O, SF_6, ^{222}Rn and biweekly integrated sampling of $\Delta^{14}C$, as presented by van der Laan et al. (2009a, 2010). Basic meteorological conditions are monitored at all sites, including wind speed and direction, temperature, atmospheric pressure and relative humidity. The main wind direction is between southwest and west (van der Laan et al., 2009b),
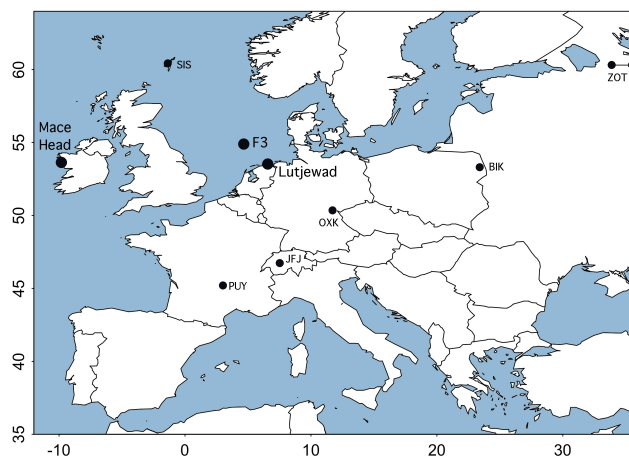

Fig. 1. Location of the three stations from which the flasks have been sampled: Lutjewad, Mace Head and F3. Also shown are the locations of other European measurements which are used for comparison. These are: Ochsenkopf (OXK), Bialystok (BIK), Shetland Islands (SIS), Zotino (ZOT), Puy de Dôme (PUY) and Jungfraujoch (JFJ).

which implies a continental contribution with the main wind direction.

Mace Head atmospheric research station (53°20′ N, 9°54′ W) is located on the west coast of Ireland. With the prevalent wind direction from the western section, the station is ideal for sampling background air masses originating from the Atlantic Ocean (e.g. Derwent et al., 2002). Further details on Mace Head atmospheric research station are provided by e.g. Derwent et al. (2002) and Jennings et al. (1993). At Mace Head air samples were collected from 35 m a.s.l. during restricted baseline conditions (Bousquet et al., 1996).

The sea based measurement station F3 is situated on a North Sea oil and gas platform (54°51′ N, 4°44′ E), 200 km north of the Dutch coast. The platform produces oil and gas and is operated by Gaz de France (GdF Suez). The F3 station contains an automated flask sampler similar to that at Lutjewad, as well as a set-up for continuous monitoring of atmospheric CO_2 and O_2 concentrations (van der Laan-Luijkx et al., 2010). The continuous measurements of O_2 are performed with an Oxzilla II instrument (fuel cells) and CO_2 is measured using infrared absorption (CarboCaps, Vaisala). The air inlets of both the flask autosampler and the continuous measurement setup are situated on the top deck at 46 m a.s.l. The depth of the North Sea at this location is 44 m and the prevalent wind direction at F3 is southwest. Flasks are filled when the wind direction is between south and west. We thereby sample mainly the coastal marine section of the north-western part of the European continent.

3 Methods

3.1 Flask sampling and measurement techniques

Since the end of 2000 weekly air samples are taken at Lutjewad from the air inlet at the top of the tower (60 m) using a remotely controlled flask sampler (Neubert et al., 2004). This sampler fills 2.5 l flasks with dried air at a specified time interval and accommodates the possibility to fill up to 20 flasks. The sampler consists of a manifold with valves to select the individual flasks for filling and a cryocooler for air drying. The automated air drying system is described by Neubert et al. (2004) with additional information given by van der Laan-Luijkx et al. (2010). Each flask is flushed with dried air for 60 min before the automated system closes the flask and continues to the next flask. At F3 the same system is used, but due to space limitations a maximum of 10 flasks is connected to the system at a time. The glass flasks used have glass valves from Louwers (Hapert, the Netherlands) with viton o-rings and ball and cup joint connections (Rotulex). The valves are operated using electric valve actuators designed at the Centre for Isotope Research (CIO, Groningen, the Netherlands). At Mace Head, identical flasks are manually filled in pairs every week. The cryogenically dried air is sucked in the flasks which are filled to atmospheric pressure.

All flasks are analyzed in the CIO laboratory for their concentrations[1] of CO$_2$, CH$_4$ and CO, as well as for δO$_2$/N$_2$, δ^{13}CO$_2$, δCO^{18}O and Δ^{14}CO$_2$. δO$_2$/N$_2$ is measured using a Micromass Optima dual inlet isotope ratio mass spectrometer (DI-IRMS), in a similar manner as Bender et al. (1994). The concentrations of CO$_2$, CH$_4$ and CO are measured using a Hewlett-Packard gas chromatograph (GC), model 6890, comparable to the setup described by Worthy et al. (2003). More details on the measurement instruments are presented by Sirignano et al. (2010).

3.2 O$_2$/N$_2$ calculations and calibration

Changes in the atmospheric O$_2$ concentration are usually reported as the changes in the ratio of O$_2$ to N$_2$. As the atmospheric N$_2$ concentration is much less variable, the changes in the O$_2$/N$_2$ ratio mainly represent changes in the O$_2$ concentration. Unlike the O$_2$ concentration, the O$_2$/N$_2$ ratio is insensitive to the changes in other atmospheric gases, such as CO$_2$. Changes in the O$_2$/N$_2$ ratio of a sample are expressed as relative deviations from a known reference gas, as shown in Eq. (1) (Keeling and Shertz, 1992).

$$\delta(O_2/N_2) = \frac{(O_2/N_2)_{sample}}{(O_2/N_2)_{reference}} - 1 \tag{1}$$

For natural air, the δO$_2$/N$_2$ values are relatively small and are therefore multiplied with 10^6 and expressed in per meg.

[1] In this paper the more correct term mixing ratio has been substituted by concentration to avoid confusion with the term O$_2$/N$_2$ ratio.

While mass spectrometers measure δO$_2$/N$_2$ directly, other methods measure the O$_2$ concentration. When measuring the O$_2$ concentration directly, dilution by changes in the CO$_2$ concentration requires a correction and therefore simultaneous measurements of the CO$_2$ concentration. Equation (2) (Kozlova et al., 2008; Stephens et al., 2003) shows the relationship between changes in the O$_2$ concentration and changes in δO$_2$/N$_2$.

$$\delta(O_2/N_2) = \frac{\delta XO_2 + (\Delta CO_2 \cdot S_{O_2})}{(1 - S_{O_2}) \cdot S_{O_2}} \text{(in per meg)} \tag{2}$$

Here, $S_{O_2} = 0.20946$ (Machta and Hughes, 1970) represents the standard mole fraction of O$_2$ in air and δXO_2, ΔCO_2 and $\delta O_2/N_2$ are the changes in the O$_2$ mole fraction, the CO$_2$ concentration and the O$_2$/N$_2$ ratio, respectively. A change of 1 ppm in the O$_2$ mole fraction without any concurrent change in CO$_2$ therefore causes a change of 6.04 per meg in δO$_2$/N$_2$. However, in case 1 ppm of O$_2$ molecules is removed from an air package while the same amount of CO$_2$ molecules is added this causes a change of 4.77 per meg in δO$_2$/N$_2$.

Earlier work by Sirignano et al. (2010) showed the atmospheric O$_2$ concentrations from Lutjewad and Mace Head presented on the internally used CIO scale, stating the need for an adaptation to an internationally used scale for intercomparison of the measurement accuracy as well as data comparison. The complete data series was recalibrated using three cylinders spanning from -805 to -258 per meg purchased from the Scripps Institution of Oceanography (SIO). The mass spectrometer measures each sample twice against a machine reference gas – i.e. the reference in Eq. (1). Besides the samples, working gas cylinders were measured following an identical procedure as for the samples. Each measurement gives the difference between the sample or working gas and the machine reference gas. The calibration procedure included a drift correction of this difference based on the measurements of a suite of working cylinders against the machine reference gas. The amount of working gas cylinders used has increased over time from one cylinder to four, which makes the latest data more accurate than the earlier data. During the start-up phase of the measurements, the machine reference gas has been changed several times, requiring a scale conversion for each change. The SIO primary cylinders were measured only against the current machine reference gas, which makes the data of samples measured (i.e. not necessarily sampled) after 2006 the most accurate. The combined uncertainty in the measurements of the flask samples varies between 6 per meg for the latest measurements to 15 per meg in the initial measurement periods. The used procedures and further details on each measurement period are extensively described in van der Laan-Luijkx (2010).

For the CO$_2$ concentration, each flask is measured at least two times on our GC in order to enhance the measurement precision. A working standard is measured after every second sample measurement, and the measurement sequence includes a target cylinder for quality control. The GC

measurements are calibrated with a suite of standards purchased from the Earth System Research Laboratory (ESRL) of the National Oceanic and Atmospheric Administration (NOAA). The final CO_2 concentrations of the flask samples is expressed in ppm on the World Meteorological Organization (WMO) X2007 scale.

3.3 Atmospheric Potential Oxygen (APO) and APO*

Stephens et al. (1998) have defined the tracer Atmospheric Potential Oxygen (APO), as shown in Eq. (3).

$$\delta APO = \delta O_2/N_2 + \frac{1.1 \cdot (CO_2 - 350)}{S_{O_2}} \text{ (per meg)} \qquad (3)$$

APO is the sum of $\delta O_2/N_2$ plus 1.1 times the CO_2 concentration, with 1.1 being the global average stoichiometric ratio (α_B) between O_2 and CO_2 in photo-synthesis and respiration processes (Severinghaus, 1995). S_{O_2} is the standard mole fraction of O_2 in air. An arbitrary reference of 350 ppm is subtracted from the CO_2 concentration, as used on the SIO per meg scale for APO (Manning and Keeling, 2006). The definition implies that APO is unaffected by activity of land biota and is therefore sensitive principally to ocean-atmosphere exchange of O_2 and CO_2, but also still partly to fossil fuel combustion and its specific oxidation ratio (OR $= -\Delta O_2 / \Delta CO_2$). The global average OR for fossil fuel is $\alpha_F = 1.4$ (Keeling, 1988b). Therefore the APO on average still includes 0.3 times the fossil fuel combustion contribution, which can be seen from the global budgets for CO_2, O_2 and APO (in moles) in Eq. (4) through (6) (Manning and Keeling, 2006).

$$\Delta CO_2 = F - B - O \qquad (4)$$

$$\Delta O_2 = -\alpha_F F + \alpha_B B + Z \qquad (5)$$

$$\Delta APO = \Delta O_2 + \alpha_B \Delta CO_2 = (\alpha_B - \alpha_F)F - \alpha_B O + Z \qquad (6)$$

Here, ΔCO_2 and ΔO_2 are the changes in the atmospheric concentration of CO_2 and O_2 respectively, expressed in moles. F is the CO_2 emission to the atmosphere originating from fossil fuel combustion and cement manufacture. B is the net uptake of CO_2 from the atmosphere by the terrestrial biosphere. O is marine CO_2 uptake and Z is the net marine O_2 exchange (where a positive sign indicates addition of O_2 to the atmosphere). As both the CO_2 fossil fuel source and the terrestrial biospheric CO_2 sink are directly coupled to the changes in the O_2 concentration, they are included in the relationship for O_2 with their respective molar exchange ratios (α_B and α_F respectively). The marine processes involving CO_2 and O_2 are not coupled, and they are therefore represented by different symbols (O and Z). The relationship for APO as represented in (6) shows that APO is unaffected by terrestrial biosphere activity.

As APO is defined to estimate marine CO_2 uptake, the remaining influence of fossil fuel combustion should be accounted for. Sirignano et al. (2010) therefore suggest the use of a modified version of APO, named APO*, which is defined in Eq. (7) and is truly only sensitive to ocean-atmosphere exchange.

$$\Delta APO^* = \Delta APO - (\alpha_B - \alpha_F)F \qquad (7)$$

The oxidative ratio for fossil fuel combustion (α_F) varies over the globe, depending on the types of fossil fuels that are used in each country. The oxidative ratios for the individual fossil fuel types are: 1.17 for coal, 1.44 for oil and 1.95 for natural gas (Keeling, 1988a). Biofuels have the lowest OR, around 1.1, which is identical to the ratio for terrestrial biospheric release. Therefore combustion of biofuels is also removed from the APO signal like the terrestrial biosphere. In the Netherlands the fossil fuel OR is higher than average (around 1.7 Sirignano et al., 2010), because of the high share of natural gas. The use of natural gas varies significantly within the different seasons and is especially high in winter as it is mainly used for heating purposes. We have used a modelling study to estimate the influence of regional deviations from the global average OR for fossil fuel for our three measurement locations, which is described in the following section.

3.4 REMO

The REgional MOdel (REMO) (Chevillard et al., 2002; Langmann, 2000) is an atmospheric transport model covering in this study the area north of 30° N, which includes the European continent. The model's grid resolution is $0.5° \times 0.5°$ in a rotated spherical coordinate system, corresponding to a grid cell resolution of approximately 55×55 km. The atmosphere is divided in 20 vertical levels, of which we use the lowest level between 0 and 65 m, corresponding to the height of our sampling sites. The initial and lateral boundary conditions for the meteorology were based on the ECMWF (European Centre for Medium-Range Weather Forecasts) analysis and for CO_2 and APO the TM3 global transport model was used. The surface fluxes for the oceanic APO were calculated from TM3 inversion of atmospheric CO_2 and O_2 concentrations (Rödenbeck et al., 2008). For the fossil fuel part of APO, hourly fluxes of CO_2 emissions and O_2 uptake from the CO_2 release and Oxygen uptake from Fossil Fuel Emissions Estimate (COFFEE) dataset (Steinbach et al., 2010) were used as input for the model. This dataset combines CO_2 emissions from the Emission Database for Global Atmospheric Research (EDGAR) inventory version 3.2 (Olivier and Berdowski, 2001) extrapolated to 2006 using BP fossil fuel consumption data at national level (available at: http://www.bp.com/ statisticalreview) with fossil fuel type specific oxidative ratios derived from fuel consumption data from the UN energy statistics (http://data.un.org). Seasonal and diurnal variations of the emissions were included based on time profiles available in the EDGAR database. Figure 2a shows the global distribution of the oxidative ratios from fossil fuel combustion for 2006 and Fig. 2b shows the region of our sampling
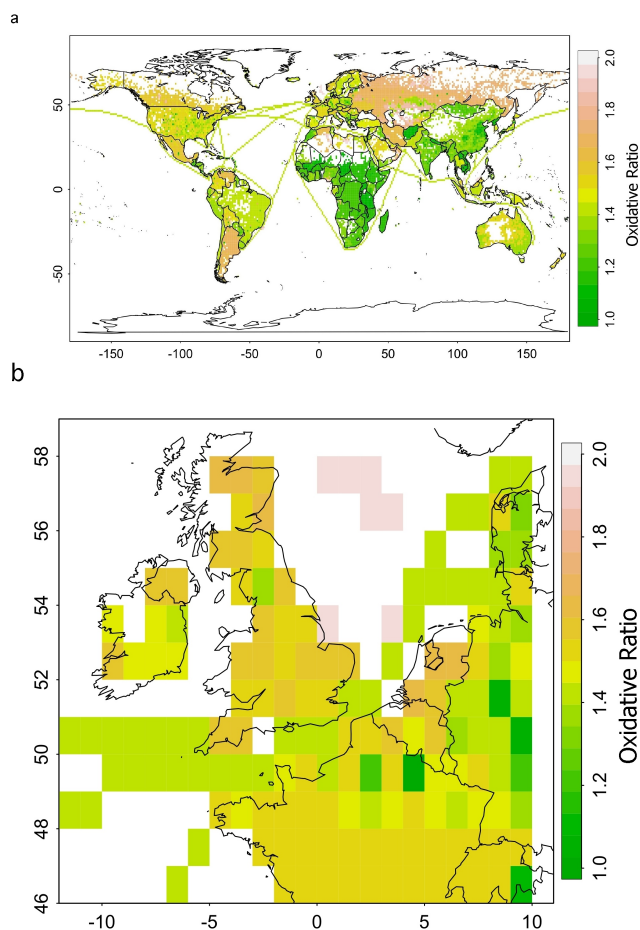
Fig. 2. The global distribution of the oxidative ratios from fossil fuel combustion **(a)** and the regional distribution at our sampling locations in more detail **(b)** (Steinbach et al., 2010). These are the emissions based fossil fuel ORs per grid cell and are used as an input in the used regional model study. White grid cells indicate that no data is available in the EDGAR database. For Lutjewad the average of the two grid cells just below the actual position has therefore been used in this paper.

locations in more detail (Steinbach et al., 2010). The oxidative ratios obtained from these datasets for the fossil fuel emissions at the locations of our sites, averaged over 2006, are: 1.64 for Lutjewad, 1.49 for Mace Head and 1.44 for F3. As Lutjewad is located in a grid cell with no data available in the EDGAR database, we have used the average of the data from the two grid cells south of the actual location (the cells to the north represent shipping routes in EDGAR and are therefore less representative). These oxidative ratios are based on the emission information in the specific grid cell of the described datasets, and are not necessarily the same as the observed atmospheric O_2/CO_2 ratios, which are subject to atmospheric transport and mixing. The influence of transport and mixing is taking into account in this study by using the O_2/CO_2 ratio resulting from the REMO simulations, hereinafter referred to as perceived OR.

4 Results

4.1 CO_2 and O_2

Flasks have been filled with air at Lutjewad since October 2000, at Mace Head since December 1998 and at the F3 North Sea platform since June 2006. The data series for the atmospheric concentrations of O_2 and CO_2 from flask samples between 2000 and 2005 from Lutjewad and Mace Head have been presented by Sirignano et al. (2010). In this section we present the follow-up of this work with extended data series until 2009. In addition, for F3 half-hourly averaged continuous measurements are available from September 2008 to June 2009 as described by van der Laan-Luijkx et al. (2010). The continuous O_2 record presented in that paper has also been converted to the internationally used Scripps scale – as the flask data – to be able to make a direct comparison.

Flasks which were suspected to have been contaminated (e.g. by leaks in the sampling or measurement system or due to long storage of the flasks; Sturm et al., 2004) have been removed from the data set, as well as those flasks which were marked as locally influenced samples or samples with a continental trajectory. At Lutjewad these samples were identified using the concentration of ^{222}Rn, which has been measured simultaneously at Lutjewad since 2005. ^{222}Rn is a radioactive noble gas emanating from soils. The emissions of ^{222}Rn from oceans is very small, therefore these characteristics can be used to determine whether the air masses have been influenced by continental emissions. Therefore, all flasks with a ^{222}Rn concentration higher than $3\,\text{Bq/m}^3$ are disregarded as they represent air with continental influences and are not background air. As we did not measure ^{222}Rn before 2005 at Lutjewad, the ^{222}Rn concentrations have been correlated with the CO concentrations at Lutjewad, leading to an exclusion of the flask samples containing CO concentration higher than 200 ppb. We subsequently used this criterion for the exclusion of flask samples at Mace Head and F3. For Mace Head only a small amount of flasks were excluded as they were sampled during restricted baseline conditions.

For both O_2 and CO_2 the data have been filtered, based on a fit through the data points. The used fit is a linear combination of a three harmonic seasonal component and a linear trend. Data points with residuals larger than 2.5 times the standard deviation from the original fit have been excluded. This process has been iterated until no further outliers were identified. For F3 we have used the data from both the flasks and the continuous measurements to improve the quality of the fit (compared to fitting flask data only). On average around 10% of the data was excluded by applying the filtering procedure to each of the data series. Our fitting strategy is slightly different from that used in Sirignano et al. (2010) in that we have chosen a linear trend fit instead of a Loess trend fit (Cleveland and Devlin, 1988). The Loess trend fit is very sensitive to unevenly time-distributed data. As our data series have several
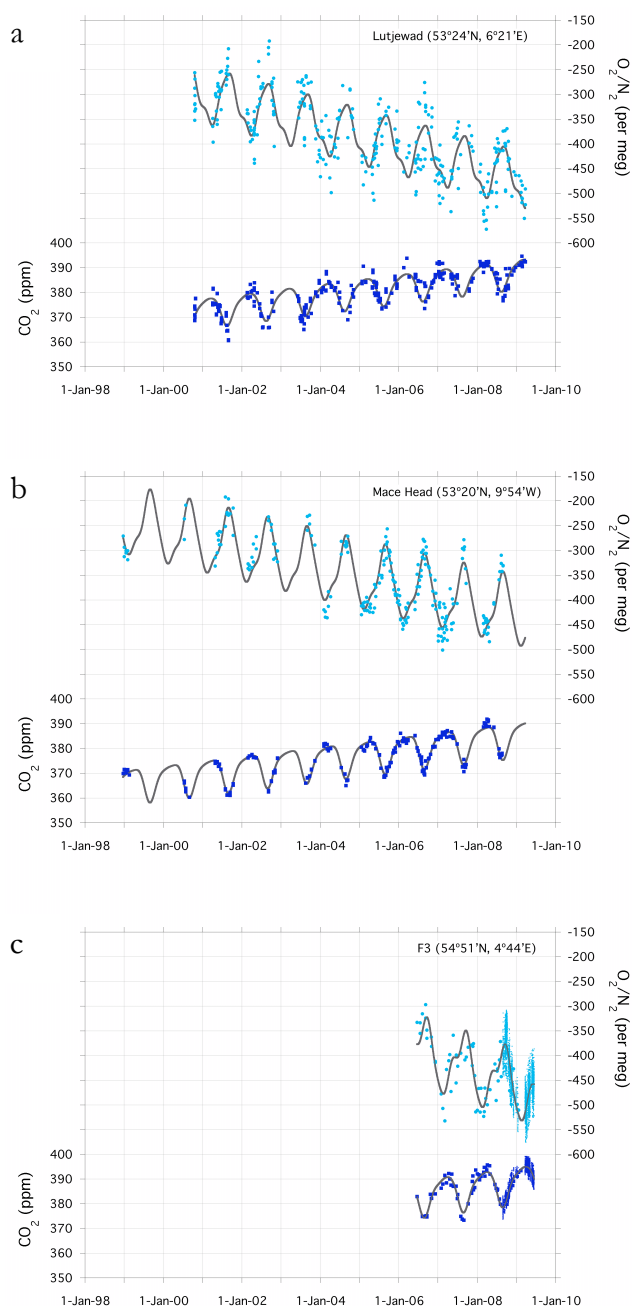
Fig. 3. Observations of the atmospheric O_2 (lighter circles) and CO_2 (darker squares) concentrations at station Lutjewad **(a)**, Mace Head **(b)** and F3 **(c)** during 1998–2009, based on flask measurements (and continuous measurements for F3). The fits through the data points are a combination of a three harmonic function and a linear trend.

Fig. 4. Trend fits of CO_2 **(a)** and O_2 **(b)** at Lutjewad (solid black line), Mace Head (dashed black line) and F3 (solid blue line) during 1998–2009, based on flask measurements (and continuous measurements for F3). The fits are a linear combination of a three harmonic function and a linear trend through the data points (in Fig. 3). The CO_2 trends of the three measurement locations are shown in comparison to the CO_2 background reference concentration according to GLOBALVIEW-CO_2 (2008) (solid grey line) at latitude 53° N. The increasing gradients between Mace Head and Lutjewad are visible for both CO_2 and $\delta O_2/N_2$.

gaps and more (not-excluded) flask samples in certain periods, the Loess fit does not provide valid information on the trend variability.

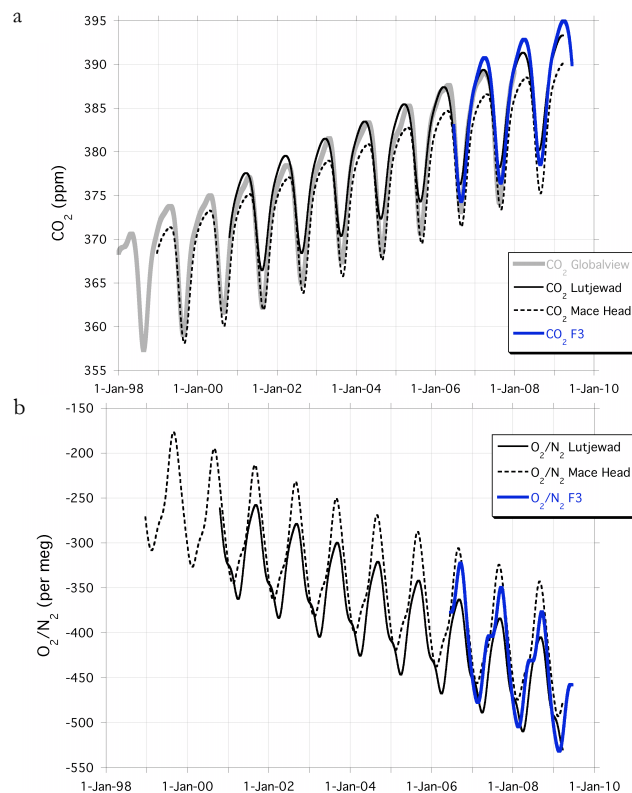Figure 3 shows the observations from each station for CO_2 and O_2 respectively. The expected seasonal patterns are clear in the data series of all three sites as well as the long term trends, slowly increasing for CO_2 and a concurrent decreasing trend for O_2. The observed signals for O_2 and CO_2 from Lutjewad and also F3 show a higher degree of variability compared to Mace Head. These stations are more influenced by local and regional sources and sinks of CO_2 and O_2 (e.g. terrestrial biosphere and fossil fuel emissions) and the sampling and filtering procedures do not adequately exclude these disturbances. The regional influence at Lutjewad has been presented by van der Laan et al. (2010) and is used to estimate national fossil fuel CO_2 emissions. The observations from our three stations have been fitted and an overview of the obtained fit parameters for the respective complete sampling periods is presented in Table 1. A comparison of the obtained fit results of our three measurement locations is shown in Fig. 4. The three harmonic fits of the detrended seasonal cycles for both CO_2 and $\delta O_2/N_2$ are shown in Fig. 5.

Table 1. CO_2 and O_2 trend and seasonality based on the fit of the data sets from each measurement site: Lutjewad, Mace Head and F3. The used fit is a linear combination of a linear trend and a 3-harmonic seasonal component.

	Lutjewad	Mace Head	F3
Trend CO_2 (ppm/year)	1.97 ± 0.07	1.90 ± 0.04	2.11 ± 0.04
Trend $\delta O_2/N_2$ (per meg/year)	-21.0 ± 0.9	-18.5 ± 0.7	-27.1 ± 0.6
Trend APO (per meg/year)	-10.6 ± 0.7	-8.4 ± 0.7	-13.2 ± 0.5
Amplitude CO_2 (ppm)	12.0 ± 0.6	14.0 ± 0.3	15.2 ± 0.1
Amplitude $\delta O_2/N_2$ (per meg)	114 ± 8	142 ± 6	144 ± 2
Amplitude APO (per meg)	64 ± 6	74 ± 6	111 ± 2
Day of maximum CO_2	72 (13 Mar)	107 (17 Apr)	84 (25 Mar)
Day of minimum CO_2	229 (17 Aug)	242 (30 Aug)	240 (28 Aug)
Day of minimum $\delta O_2/N_2$	90 (31 Mar)	42 (12 Feb)	49 (19 Feb)
Day of maximum $\delta O_2/N_2$	252 (9 Sep)	243 (31 Aug)	263 (19 Sep)
Day of minimum APO	84 (25 Mar)	40 (10 Feb)	15 (16 Jan)
Day of maximum APO	255 (12 Sep)	243 (31 Aug)	171 (20 Jun)
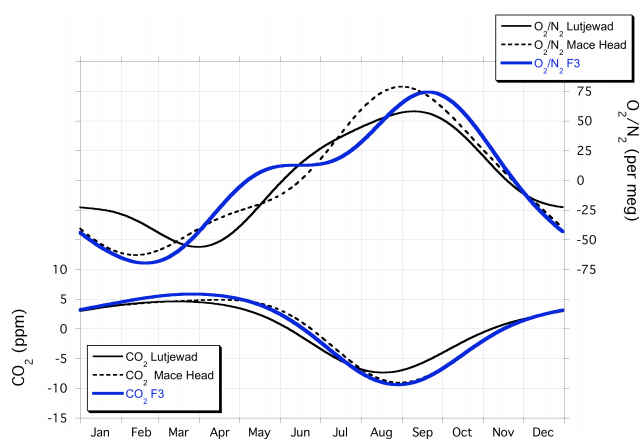
Fig. 5. The de-trended seasonal patterns of CO_2 and O_2 at station Lutjewad (black solid line), Mace Head (black dashed line) and F3 (blue solid line) during 1998–2009, based on flask measurements (and continuous measurements for F3).

The long term trend in the Lutjewad CO_2 concentration (Fig. 3a) is estimated at 1.97 ± 0.07 ppm/year for CO_2 and -21.0 ± 0.9 per meg/year for $\delta O_2/N_2$. At Mace Head the long term trend is found to be 1.90 ± 0.04 ppm/year for CO_2 and -18.5 ± 0.7 per meg/year for $\delta O_2/N_2$. Since the data series at the F3 platform is only 3 years the long term trends cannot provide as accurate information on the trends, which are estimated at 2.11 ± 0.04 ppm/year for CO_2 and -27.1 ± 0.6 per meg/year for $\delta O_2/N_2$ (the errors given are the fit errors and because of the short length of the record they do not necessarily reflect the total error including systematic and measurement errors). Thanks to the longer sampling period, our trend estimates are now much more accurate than those presented by Sirignano et al. (2010), but the results correspond well to each other within the uncertainty

range. The long-term trends for CO_2 and $\delta O_2/N_2$ for other European sites are included in Table 2. Their locations are included in Fig. 1 using abbreviated station names. The CO_2 trends at all sites are close to each other at about 2 ppm/year, except for Puy de Dôme. The trends for $\delta O_2/N_2$ are all close to -20 per meg/year, except for Jungfraujoch.

For Lutjewad we find a seasonal (peak-trough) amplitude of 12.0 ± 0.6 ppm for CO_2 and 114 ± 8 per meg for $\delta O_2/N_2$. For Mace Head we find a seasonal amplitude of 14.0 ± 0.3 for CO_2 and 142 ± 6 per meg for $\delta O_2/N_2$. For F3 we find a seasonal amplitude of 15.2 ± 0.1 ppm for CO_2 and 144 ± 2 per meg for $\delta O_2/N_2$. Even though the record at F3 is still short, the quality of the seasonal component in the fit is considerably higher here, thanks to the continuous data. Figure 4a shows a comparison of the fits of CO_2 from our three measurement locations to the marine background layer reference from the GLOBALVIEW-CO_2 (2008) database for the same latitude (53° N). From this figure we can conclude that the fits of the Lutjewad, Mace Head and F3 data correspond well to the GLOBALVIEW-CO_2 signal when comparing the timing of the growing season. The sharp decrease marking the uptake of CO_2 by the land biota and the slower increase indicating the end of the growing season are clearly reflected in all fits and compare well to that of GLOBALVIEW-CO_2. The CO_2 signal from Lutjewad follows the GLOBALVIEW-CO_2 signal well, except for the depth of the troughs in the growing season. Also in comparison to previous studies, the amplitude of the signal from Lutjewad is likely estimated too low based on our record. Sirignano et al. (2010) found a seasonal amplitude of 16.1 ± 0.4 ppm and van der Laan et al. (2009a) obtained 14 ppm from continuous observations. Our obtained seasonal amplitude for Mace Head does correspond well to that in Sirignano et al. (2010). The fact that our obtained amplitude for Lutjewad is lower than in both other studies and the GLOBALVIEW-CO_2 background reference is likely caused by inadequate representation of the seasonal

Table 2. CO$_2$, δO$_2$/N$_2$ and APO trend and seasonality from Lutjewad and Mace Head flask samples and for F3 from a combination of flask samples and continuous observations in comparison to observations from other European measurement locations. The error bars for the trends and amplitudes presented in this work are given in Table 1.

Location	Trend (per year)			Amplitude			Measurement Period
	CO$_2$ (ppm)	O$_2$/N$_2$ (per meg)	APO	CO$_2$ (ppm)	O$_2$/N$_2$ (per meg)	APO	(Flasks or Continuous) Reference
Lutjewad 53°24′ N, 6°21′ E	1.97	−21.0	−10.6	12.0	114	64	2000–2009 (F) (this work)
Mace Head 53°20′ N, 9°54′ W	1.90	−18.5	−8.4	14.0	142	74	1998–2009 (F) (this work)
F3 54°51′ N, 4°44′ E	2.11	−27	−13	15.2	144	111	2006–2009 (C and F) (this work)
Ochsenkopf 50°02′ N, 11°48′ E	1.6	−16	−9.7	15.5	135	43	2006–2008 (C) Thompson et al. (2009)
Bialystok 53°13′ N, 23°01′ E	2.0	−23	x	25	161	43	2005–2008 (C) Popa et al. (2009)
Shetland Islands 60°17′ N, 1°17′ W	2.2	−19	−7.2	15.4	163	95	2004–2008 (F) Kozlova et al. (2008)
ZOTTO 60°48′ N, 89°21′ E	2.0	x	x	26.6	134	51	2005–2007 (C) Kozlova et al. (2008)
Puy de Dôme 45°46′ N, 2°58′ E	1.2	−17	x	16.1	118	45	2004–2008 (F) Uglietti (2009)
Jungfraujoch 46°33′ N, 7°59′ E	1.8	−13	−5 to −22	9.9	76	21	2006–2008 (F) Uglietti (2009)

cycle in the fit. Figure 3a shows that several data points indicate a lower summer CO$_2$ value for Lutjewad which are not well reflected in the fit due to a too low sampling frequency in the narrow trough periods. The seasonal amplitude at Lutjewad as estimated from the fit is therefore likely to be higher than that presented in Table 1. Since the period with the lowest yearly CO$_2$ values is relatively short, a higher sampling frequency is recommendable for this period during summer. Figure 5 shows more clearly than Fig. 3 that the start of the growing season is observed earlier at Lutjewad (and also at F3) than at Mace Head, showing that the influence of the land biota is more visible in the Lutjewad signal. As Lutjewad is influenced by continental air masses with southern and eastern winds, the signal is frequently influenced by local (or continental) anthropogenic sources, concealing the terrestrial biosphere signal. Figure 4b shows the same comparison between the fit results of the data from the three locations for δO$_2$/N$_2$ (a δO$_2$/N$_2$ GLOBALVIEW background reference is currently not available).

The seasonal amplitudes for CO$_2$ and δO$_2$/N$_2$ from other stations within Europe are presented in Table 2. It can be seen that the highest seasonal amplitudes for CO$_2$ are found at the eastern continental sites Bialystok and ZOTTO. The seasonal cycles from Mace Head, F3 and Lutjewad (when taking into account that the estimate of 12.0 is likely to be too low) compare best to observations from Ochsenkopf and the Shetland Islands. The Ochsenkopf amplitudes are given

from the highest level in the tower (163 m) which is generally above the boundary layer, which decreases local influences. Jungfraujoch has a significantly lower CO$_2$ seasonal amplitude due to its high altitude of 3580 m a.s.l. which causes it to be far above the planetary boundary layer and thereby sampling European background air masses. The amplitudes of the seasonal cycles of δO$_2$/N$_2$ from our three sites vary more than for CO$_2$. Again, the seasonal amplitude of Lutjewad is probably underestimated; therefore Lutjewad compares best to Ochsenkopf and ZOTTO regarding their seasonal amplitudes. The seasonal amplitudes at Mace Head and F3 are slightly higher, 142 and 144 per meg, with both stations sampling only the marine sectors. The seasonal amplitude at Jungfraujoch is again much lower due to the sampled background air masses.

4.2 APO

For each measurement site, the atmospheric potential oxygen (APO) has been calculated using the observed CO$_2$ and O$_2$ concentrations and Eq. (3). The results for APO are shown in Fig. 6 for Lutjewad (a), Mace Head (b) and F3 (c) and are fitted with a linear combination of a three harmonic function and a linear trend, like for CO$_2$ and δO$_2$/N$_2$ (the fit parameters are shown in Table 1). The seasonal amplitudes of APO are roughly half of that of δO$_2$/N$_2$, as expected. The amplitudes for our three measurement sites are:
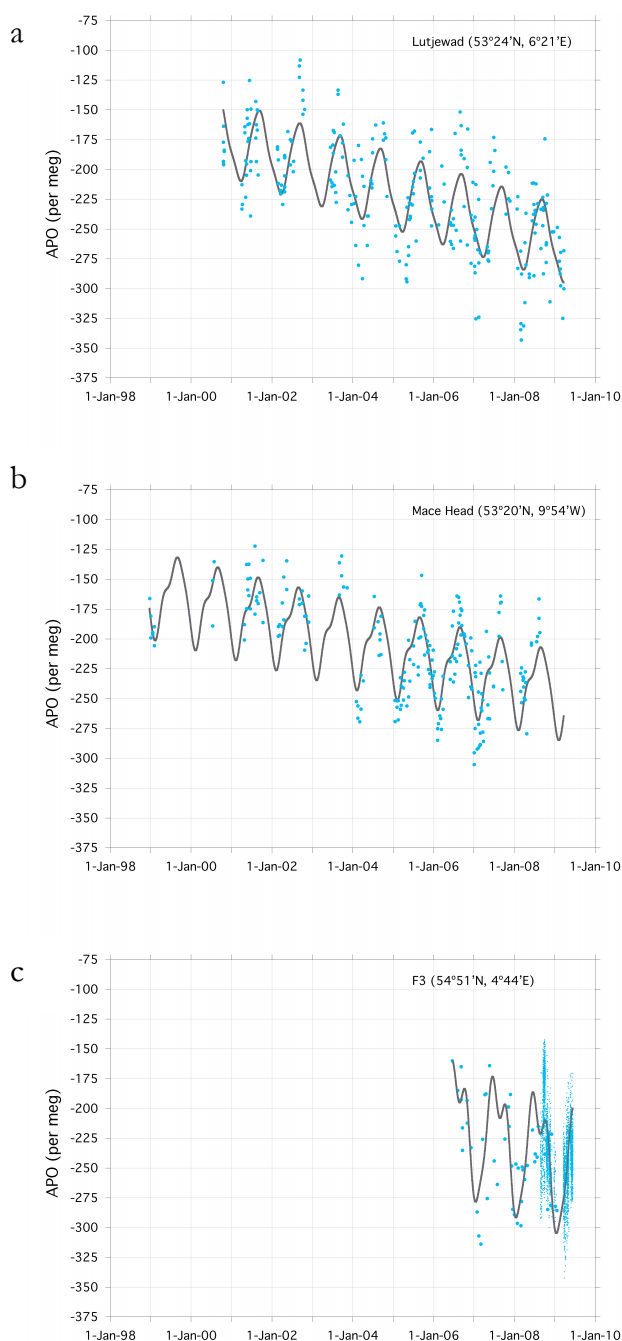
Fig. 6. Observations of the Atmospheric Potential Oxygen (APO) at station Lutjewad (**a**), Mace Head (**b**) and F3 (**c**) during 1998–2009, based on flask measurements (and continuous measurements for F3). The fits through the data points are a combination of a three harmonic function and a linear trend.

64 ± 6 per meg for Lutjewad, 74 ± 6 per meg for Mace Head and 111 ± 2 per meg for F3. The annual long term trend for each site is: −10.6 ± 0.7 per meg/year for Lutjewad and −8.4 ± 0.7 per meg/year for Mace Head. The data series for F3 is not long enough yet to provide precise information on the trend, which is roughly estimated at −13.2 ± 0.5 per

meg/year (again, the errors given are the fit errors and are higher when considering the total error). The APO fit can also be calculated using the respective CO$_2$ and δO$_2$/N$_2$ fits, this does not yield significantly different results.

For comparison, the seasonal amplitudes and annual trends for APO from other European stations are shown in Table 2. The seasonal amplitudes at our sampling sites are higher than those from most other continental European stations. As APO primarily reflects the oceanic signal, the difference between the continental sites and the coastal marine sites is expected. The APO signal at the Shetland Islands also shows a higher amplitude. The long-term trends are not available for all sites, mainly because of the short time series.

4.3 Mace Head – Lutjewad gradient

From the observed CO$_2$ and O$_2$ signals and their trend fits as presented in the previous sections we find an offset between Mace Head and Lutjewad. The offset for CO$_2$ and O$_2$ are changing over time during the course of our observational period. A calibration problem to explain the difference in these trends is excluded based on the fact that flask samples from both locations are measured on the same instrument in the same laboratory. The Mace Head signal is also showing a significant offset from the marine background signal GLOBALVIEW-CO$_2$, especially during winter. The CO$_2$ excess at Lutjewad compared to Mace Head increases with 0.5 ppm during 2001–2008. Ramonet et al. (2010) present the difference between the CO$_2$ concentration at Mace Head and nine other measurement stations in continental Europe. During the period 2000–2005 they observe an upward trend in ΔCO$_2$ (i.e. [CO$_2$]$_{measurement\ site}$ − [CO$_2$]$_{Mace\ Head}$). Compared to 1995–2000 they obtained an increase in ΔCO$_2$ by up to 2 ppm. Our calculated increase in the CO$_2$ excess at Lutjewad of 0.5 ppm fits well into the general picture presented by Ramonet et al. (2010).

Additionally, we obtained a change in the difference between Mace Head and Lutjewad for O$_2$. The O$_2$ deficit at Lutjewad compared to Mace Head increases by 20 per meg over the period of our observations (2001–2008). Consistently with the obtained increasing CO$_2$ excess and O$_2$ deficit at Lutjewad compared to Mace Head, the APO deficit also increases. As the terrestrial biosphere is removed from the APO signal and the fact that the gradient in O$_2$ is still present in APO, this implies a relation with either the ocean, fossil fuel combustion or general atmospheric conditions.

Ramonet et al. (2010) attributed their obtained increase in ΔCO$_2$ to a combination of a shallower boundary layer height over the continent and regional changes in fossil fuel emissions. Based on our obtained increase in CO$_2$ excess of 0.5 ppm at Lutjewad and the global average fossil fuel oxidative ratio of 1.4, an increase of the O$_2$ deficit of 3.4 per meg would be expected. The large difference with our observed increasing O$_2$ deficit implies other major contributions to these changes.
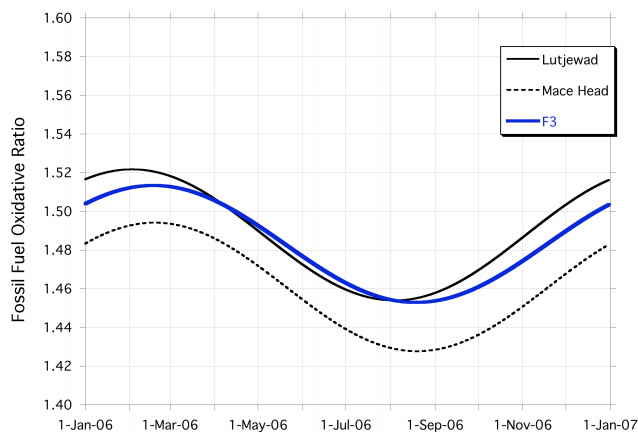
Fig. 7. Fit of the modelled data of fossil fuel CO_2 and O_2 for 2006 expressed as the perceived fossil fuel oxidative ratio (OR) for our three measurement locations using REMO. The fit shows the seasonal variability in the average OR for each location during the course of the year as well as the spatial variability between the three sites. The OR at all sites differs significantly from the global mean OR of 1.4 as well as from its local emission based OR (EDGAR) as shown in Fig. 2a.

Another possible contribution to the increasing CO_2 excess and O_2 deficit at Lutjewad compared to Mace Head could also originate from changes in the CO_2 uptake by the North Atlantic. Oceanographic research has shown that the North Atlantic CO_2 sink has varied substantially over the past years, and has also decreased during certain periods (e.g. Corbière et al., 2007; Schuster and Watson, 2007; Watson et al., 2009). Furthermore Hamme and Keeling (2008) and Rödenbeck et al. (2008) have shown that air-sea fluxes of O_2 and CO_2 show significant interannual variations. These changes in ocean ventilation are present for both O_2 and CO_2, however in the atmosphere they are much more quickly observed for O_2 than for CO_2, due to the ocean's CO_2 buffer effect.

The final contribution to changing gradients can be found in fossil fuel emission changes. Due to the average fossil fuel oxidative ratio (OR_{ff}) of 1.4, increasing fossil fuel consumption over the continent causes a larger increase in the O_2 deficit than in the CO_2 excess. Also regional changes in the OR could cause changing gradients. An increasing share of natural gas in the fossil fuel mix over the continent would give a higher increase in the O_2 deficit compared to the CO_2 excess. That possible influence of the gradient in OR_{ff} between Mace Head and Lutjewad has been studied using the regional transport model REMO.

REMO simulations were performed for the year 2006, using the CO_2 emission data and the fuel mix specific ORs for the fossil fuel related O_2 sink, as described in Sect. 3.4. The data in Fig. 2 are used as an input for REMO. The results from REMO simulations yield the local CO_2 and O_2 concentrations at our three sampling locations. The modelled

CO_2 and O_2 signals consist of separate signals for the biosphere, ocean and fossil fuel component. Since REMO is a regional model, the perceived fossil fuel OR (i.e. the resulting $\Delta O_2/\Delta CO_2$ ratio after atmospheric transport and mixing) can be calculated directly as the ratio of the resulting atmospheric O_2 and CO_2 concentrations within a certain grid cell. For 2006 this yielded a seasonal signal for the perceived OR_{ff} (as simulated by REMO) for each of our three measurement locations as shown in Fig. 7. The perceived OR_{ff} at our three locations is structurally higher than the global average OR_{ff} of 1.4. The deviation is more pronounced in the simulations for Lutjewad and F3 than for Mace Head. The obtained average perceived OR_{ff} is 1.49 for Lutjewad, 1.46 for Mace Head and 1.48 for F3. The OR of the fossil fuel emissions in the Netherlands is highly influenced by the high natural gas share in the fossil fuel mix (as shown in Fig. 2) and this elevation continues to exist after atmospheric transport and mixing in the perceived OR_{ff}. As the CO_2 emissions and APO are transported by the model, the mixing with emissions from surrounding countries decreases the perceived fossil fuel OR at Lutjewad in comparison to the actual local emissions. The same mixing occurs at the other two sites and is obvious for F3, since the local emissions in the F3 area (according to the EDGAR database) are only influenced by international shipping, the mixing with the emissions from e.g. the Netherlands increases the OR_{ff} signal. Furthermore, the OR_{ff} of all three sites clearly shows a seasonal pattern, which has its maximum in winter, when the share of natural gas in the fossil fuel use is higher as it is the main source for (domestic) heating purposes.

The continuous difference in the oxidative ratio of the local fossil fuel emissions between the Netherlands and other countries leads to an O_2 deficit in this area which is counteracted by atmospheric transport and mixing. Therefore the magnitude of the deficit is dependent on the (interannual) variability of both the fossil fuel OR and atmospheric transport and mixing. From our study we observe that during the period of our observations this deficit has not been eliminated by transport of O_2 from adjacent regions and that the deficit at Lutjewad compared to Mace Head has increased. On the short term the fossil fuel variability influences the gradient between both locations, however it is expected that this gradient will cancel out in the long term.

4.4 Estimating global marine CO_2 uptake

We estimate the global marine CO_2 uptake using the definitions presented in Manning and Keeling (2006). The net global oceanic CO_2 uptake is calculated as shown in Eq. (8).

$$O = \left[(-\Delta(\delta APO) \times 10^{-6} \cdot S_{O_2} \cdot M_{air} \cdot M_C) + (\alpha_B - \alpha_F)F + \left(\frac{Z_{eff}}{M_C} \right) \right] \cdot \frac{1}{\alpha_B} \quad (8)$$

Where $\Delta(\delta APO)$ is the observed annual change in δAPO (in per meg), $S_{O_2} = 0.20946$ is the standard mole fraction of O_2 (Machta and Hughes, 1970), $M_{air} = 1.769 \times 10^{20}$ mol

is the number of moles of dry air in the total atmosphere and M$_C$ = 12.01 g/mol is the molar mass of carbon. The net oceanic outgassing of O$_2$ is represented as Z$_{eff}$. We use Z$_{eff}$ = 0.48 PgC/year from Manning and Keeling (2006). The global average molar stoichiometric ratios α_B and α_F are 1.1 and 1.4, respectively. For the fossil fuel emissions F we use the average annual emission, which is 7.7 PgC/year during the period 2000–2009 and 7.5 PgC/year during 1998–2009 (Boden et al., 2009).

To estimate the global marine CO$_2$ uptake we use the APO trend obtained for Mace Head, which is the station with the longest atmospheric O$_2$ record in Europe. During the measurement period the APO trend was -8.4 ± 0.7 per meg/year. As the flasks at Mace Head are sampled during restricted baseline conditions, they represent well the background situation. The trend therefore represents the global average trend, and compares well with that obtained for other regions around the globe presented in other studies (e.g. Hamme and Keeling, 2008; Manning and Keeling, 2006). Using the global average OR of 1.4, the APO trend at Mace Head gives a global oceanic CO$_2$ uptake of 1.8 ± 0.8 PgC/year.

Our estimation of the global oceanic CO$_2$ uptake of 1.8 ± 0.8 PgC/year over the period 1998–2009 agrees within the error bars with e.g. Manning and Keeling (2006). Based on the observations from La Jolla (California, USA), Alert (Canada) and Cape Grim (Australia), they found a global oceanic CO$_2$ uptake of 1.9 ± 0.6 PgC/year over the period 1990–2000 and 2.2 ± 0.6 PgC/year over the period 1993–2003. Longer time series of observations at Mace Head should be able to identify whether our lower estimate is valid and whether it is an indication of a decreasing oceanic CO$_2$ sink. The combination of the trend observed at Mace Head and longer term trends from other European background stations as well as the combination with long term continuous observations will give more information on the spatial and temporal variability of the global marine CO$_2$ uptake.

The APO trend obtained from the flasks sampled at Lutjewad is -10.6 ± 0.7 per meg/year during the period 2000–2008, which is significantly higher (i.e. more negative) than the trend obtained for Mace Head. For this period it is not possible to use the obtained trend for Lutjewad in global budget studies as it is to a high degree affected by regional influences. We expect that the signal at Lutjewad is heavily influenced by changes in the continent during the sampling period and that the APO trend therefore does not completely follow the global average trend. On the long term these local influences are expected to be balanced by atmospheric transport and mixing.

As discussed in Sect. 4.3 one of the possible influencing factors on the gradient between Mace Head and Lutjewad is the (difference in) the fossil fuel OR. The influence of the used OR$_{ff}$ in the global budget calculations is high. Using the global average OR$_{ff}$ of 1.4 and the APO trend observed at Mace Head we found a global marine CO$_2$ uptake of 1.8 ± 0.8 PgC/year. However, using the obtained perceived

OR$_{ff}$ of 1.46 as obtained from the REMO simulations for 2006, would yield an uptake of 1.4 ± 0.8 PgC/year. It is therefore essential that future studies focus on precisely determining the global average OR as well as its annual variability. Additionally, regional gradients such as illustrated by our observations are key to assessing regional variability in sources and sinks and therefore are a valuable input to (inverse) modelling efforts.

5 Conclusions

In this paper we have presented the CO$_2$, δO$_2$/N$_2$ and APO data series of the flask sample measurements from Lutjewad atmospheric monitoring station in the Netherlands, Mace Head atmospheric research station in Ireland and the F3 platform in the Dutch part of the North Sea together with continuous measurements from F3. With this work and that of colleagues combined, the density of the (European) δO$_2$/N$_2$ observational network is increasing gradually. These observations can be used in model efforts (both forward and inverse) to provide additional insights into the carbon cycle, also in a quantitative sense.

The records from Lutjewad and Mace Head have been used to construct the gradient in CO$_2$ and O$_2$ between Lutjewad and Mace Head. The obtained gradient fits well with the gradients observed between Mace Head and other European stations. The observed change in the CO$_2$ excess at Lutjewad compared to Mace Head is 0.5 ppm over the presented sampling period. We have also presented the δO$_2$/N$_2$ gradient between Lutjewad and Mace Head. The O$_2$ deficit at Lutjewad compared to Mace Head is gradually increasing the sampling period with 20 per meg over the total period 2001–2008. The effect on O$_2$ is much stronger than on CO$_2$, which is reflected by the fact that APO shows an increased deficit at Lutjewad as well.

We have estimated the global oceanic CO$_2$ uptake based on the Mace Head APO trend to be 1.8 ± 0.8 PgC/year. Longer data series will further improve the quality of the annual trends and the oceanic uptake. Using long-term observations of multiple locations spread around the globe will further improve the APO trend estimation and thereby improve the accuracy of the global marine CO$_2$ uptake estimate and its variability. It is also of importance that model efforts focus on independently transporting CO$_2$ and O$_2$ (instead of APO) yielding improved model based OR estimates for longer time periods.

The collection of flask samples at Lutjewad, Mace Head and F3 will be continued in the future as well as the continuous measurements at F3. For the Lutjewad atmospheric monitoring station continuous CO$_2$ data is available since 2006 (van der Laan et al., 2009a). In the near future, combined continuous measurements of δO$_2$/N$_2$ and CO$_2$ will also be available at Lutjewad.

References

Battle, M., Bender, M. L., Tans, P. P., White, J. W. C., Ellis, J. T., Conway, T., and Francey, R. J.: Global carbon sinks and their variability inferred from atmospheric O_2 and delta ^{13}C, Science, 287, 2467–2470, doi:10.1126/science.287.5462.2467, 2000.

Battle, M., Mikaloff Fletcher, S. E., Bender, M. L., Keeling, R. F., Manning, A. C., Gruber, N., Tans, P. P., Hendricks, M. B., Ho, D. T., Simonds, C., Mika, R., and Paplawsky, B.: Atmospheric potential oxygen: New observations and their implications for some atmospheric and oceanic models, Global Biogeochem. Cy., 20, GB1010, doi:10.1029/2005GB002534, 2006.

Bender, M. L., Ellis, T., Tans, P., Francey, R., and Lowe, D.: Variability in the O_2/N_2 ratio of southern hemisphere air, 1991-1994: Implications for the carbon cycle, Global Biogeochem. Cy., 10, 9–21, doi:10.1029/95GB03295, 1996.

Bender, M. L., Ho, D. T., Hendricks, M. B., Mika, R., Battle, M. O., Tans, P. P., Conway, T. J., Sturtevant, B., and Cassar, N.: Atmospheric O_2/N_2 changes, 1993–2002: Implications for the partitioning of fossil fuel CO_2 sequestration, Global Biogeochem. Cy., 19, GB4017, doi:10.1029/2004GB002410, 2005.

Bender, M. L., Tans, P. P., Ellis, J. T., Orchardo, J., and Habfast, K.: A High-Precision Isotope Ratio Mass-Spectrometry Method for Measuring the O_2/N_2 Ratio of Air, Geochim. Cosmochim. Ac., 58, 4751–4758, doi:10.1016/0016-7037(94)90205-4, 1994.

Boden, T., Marland, G., and Andres, R. J.: Global CO_2 Emissions from Fossil-Fuel Burning, Cement Manufacture, and Gas Flaring: 1751–2006., Carbon Dioxide Information Analysis Center, Oak Ridge National Laboratory, Oak Ridge, Tennessee 37831–6335, 2009.

Bousquet, P., Gaudry, A., Ciais, P., Kazan, V., Monfray, P., Simmonds, P. G., Jennings, S. G., and O'Connor, T. C.: Atmospheric CO_2 concentration variations recorded at Mace Head, Ireland, from 1992 to 1994, Phys. Chem. Earth, 21, 477–481, doi:10.1016/S0079-1946(97)81145-7, 1996.

Chevillard, A., Karstens, U., Ciais, P., Lafont, S., and Heimann, M.: Simulation of atmospheric CO_2 over Europe and western Siberia using the regional scale model REMO, Tellus B, 54, 872–894, doi:10.1034/j.1600-0889.2002.01340.x, 2002.

Cleveland, W. S. and Devlin, S. J.: Locally Weighted Regression – an Approach to Regression-Analysis by Local Fitting, J. Am. Stat. Assoc., 83, 596–610, 1988.

Corbière, A., Metzl, N., Reverdin, G., Brunet, C., and Takahashi, A.: Interannual and decadal variability of the oceanic carbon sink in the North Atlantic subpolar gyre, Tellus B, 59, 168–178, doi:10.1111/j.1600-0889.2006.00232.x, 2007.

Derwent, R. G., Ryall, D. B., Manning, A., Simmonds, P. G., O'Doherty, S., Biraud, S., Ciais, P., Ramonet, M., and Jennings, S. G.: Continuous observations of carbon dioxide at Mace Head, Ireland from 1995 to 1999 and its net European ecosystem exchange, Atmos. Environ., 36, 2799–2807, doi:10.1016/S1352-2310(02)00203-0, 2002.

GLOBALVIEW-CO_2: Cooperative Atmospheric Data Integration Project – Carbon Dioxide, CD-ROM, NOAA ESRL, Boulder, Colorado, 2008.

Hamme, R. C. and Keeling, R. F.: Ocean ventilation as a driver of interannual variability in atmospheric potential oxygen, Tellus B, 60, 706–717, doi:10.1111/j.1600-0889.2008.00376.x, 2008.

IPCC: Climate Change 2007: The Physical Science Basis. Contribution of Working Group I to the Fourth Assessment Report of the Intergovernmental Panel on Climate Change, Cambridge University Press, Cambridge, United Kingdom and New York, NY, USA, 996 pp., 2007.

Jennings, S. G., McGovern, F. M., and Cooke, W. F.: Carbon Mass Concentration Measurements at Mace Head, on the West-Coast of Ireland, Atmos. Environ. A-Gen., 27, 1229–1239, doi:10.1016/S1352-2310(02)00203-0, 1993.

Keeling, R. F.: Development of an Interferometric Oxygen Analyzer for Precise Measurement of the Atmospheric O_2 Mole Fraction, PhD Thesis, Division of Applied Sciences, Harvard University, Cambridge, Massachusetts, 178 pp., 1988a.

Keeling, R. F.: Measuring Correlations between Atmospheric Oxygen and Carbon-Dioxide Mole Fractions – a Preliminary-Study in Urban Air, J. Atmos. Chem., 7, 153–176, doi:10.1007/BF00048044, 1988b.

Keeling, R. F. and Garcia, H. E.: The change in oceanic O_2 inventory associated with recent global warming, P. Natl. Acad. Sci. USA, 99, 7848–7853, doi:10.1073/pnas.122154899, 2002.

Keeling, R. F., Najjar, R. P., Bender, M. L., and Tans, P. P.: What Atmospheric Oxygen Measurements Can Tell Us About the Global Carbon-Cycle, Global Biogeochem. Cy., 7, 37–67, doi:10.1029/92GB02733, 1993.

Keeling, R. F. and Shertz, S. R.: Seasonal and Interannual Variations in Atmospheric Oxygen and Implications for the Global Carbon-Cycle, Nature, 358, 723–727, doi:10.1038/358723a0, 1992.

Kozlova, E. A., Manning, A. C., Kisilyakhov, Y., Seifert, T., and Heimann, M.: Seasonal, synoptic, and diurnal-scale variability of biogeochemical trace gases and O_2 from a 300-m tall tower in central Siberia, Global Biogeochem. Cy., 22, GB4020, doi:10.1029/2008GB003209, 2008.

Langenfelds, R. L., Francey, R. J., Steele, L. P., Battle, M., Keeling, R. F., and Budd, W. F.: Partitioning of the global fossil CO_2 sink using a 19-year trend in atmospheric O_2, Geophys. Res. Lett., 26, 1897–1900, doi:10.1029/1999GL900446, 1999.

Langmann, B.: Numerical modelling of regional scale transport and photochemistry directly together with meteorological processes, Atmos. Environ., 34, 3585–3598, doi:10.1016/S1352-2310(00)00114-X, 2000.

Machta, L.: Oxygen depletion, in: Proceedings of the International Meeting on Stable Isotopes in Tree Ring Research, edited by: Jacoby, G. C., 125–127, 1980.

Machta, L. and Hughes, E.: Atmospheric Oxygen in 1967 to 1970,

Science, 168, 1582–1584, doi:10.1126/science.168.3939.1582, 1970.

Manning, A. C. and Keeling, R. F.: Global oceanic and land biotic carbon sinks from the Scripps atmospheric oxygen flask sampling network, Tellus B, 58, 95–116, doi:10.1111/j.1600-0889.2006.00175.x, 2006.

Manning, A. C., Keeling, R. F., and Severinghaus, J. P.: Precise atmospheric oxygen measurements with a paramagnetic oxygen analyzer, Global Biogeochem. Cy., 13, 1107–1115, doi:10.1029/1999GB900054, 1999.

Neubert, R. E. M., Spijkervet, L. L., Schut, J. K., Been, H. A., and Meijer, H. A. J.: A computer-controlled continuous air drying and flask sampling system, J. Atmos. Ocean. Tech., 21, 651–659, doi:10.1175/1520-0426(2004)021, 2004.

Olivier, J. G. J. and Berdowski, J. J. M.: Global emissions sources and sinks, in: The Climate System, edited by: Berdowski, J., Guicherit, R., and Heij, B. J., A. A. Balkema Publishers/Swets & Zeitlinger Publishers, Lisse, The Netherlands, 33–78, 2001.

Patecki, M. and Manning, A. C.: First results from shipboard atmospheric O_2 and CO_2 measurements over the North Atlantic Ocean, OCEANS 2007 – Europe, 1–6, doi:10.1109/OCEANSE.2007.4302351, 2007.

Popa, M. E., Gloor, M., Manning, A. C., Jordan, A., Schultz, U., Haensel, F., Seifert, T., and Heimann, M.: Measurements of greenhouse gases and related tracers at Bialystok tall tower station in Poland, Atmos. Meas. Tech., 3, 407–427, doi:10.5194/amt-3-407-2010, 2009.

Ramonet, M., Ciais, P., Aalto, T., Aulagnier, C., Chevallier, F., Cipriano, D., Conway, T. J., Haszpra, L., Kazan, V., Meinhardt, F., Paris, J.-D., Schmidt, M., Simmonds, P., Xueref-Remy, I., and Necki, J. N.: A recent build-up of atmospheric CO_2 over Europe. Part 1: observed signals and possible explanations, Tellus B, 62, 1–13, doi:10.1111/j.1600-0889.2009.00442.x, 2010.

Rödenbeck, C., Le Quere, C., Heimann, M., and Keeling, R. F.: Interannual variability in oceanic biogeochemical processes inferred by inversion of atmospheric O-2/N-2 and CO_2 data, Tellus B, 60, 685–705, doi:10.1111/j.1600-0889.2008.00375.x, 2008.

Schuster, U. and Watson, A. J.: A variable and decreasing sink for atmospheric CO_2 in the North Atlantic, J. Geophys. Res.-Oceans, 112, C11006, doi:10.1029/2006jc003941, 2007.

Severinghaus, J. P.: Studies of the terrestrial O_2 and carbon cycles in sand dune gases and in Biosphere 2, PhD Thesis, Columbia University, New York, 148 pp., 1995.

Sirignano, C., Neubert, R. E. M., Rödenbeck, C., and Meijer, H. A. J.: Atmospheric oxygen and carbon dioxide observations from two European coastal stations 2000–2005: continental influence, trend changes and APO climatology, Atmos. Chem. Phys., 10, 1599–1615, doi:10.5194/acp-10-1599-2010, 2010.

Sirignano, C., Neubert, R. E. M., Rödenbeck, C., and Meijer, H. A. J.: Atmospheric oxygen and carbon dioxide observations from two European coastal stations 20002005: continental influence, trend changes and APO climatology, Atmos. Chem. Phys., 10, 1599–1615, doi:10.5194/acp-10-1599-2010, 2010.

Steinbach, J., Gerbig, C., Rödenbeck, C., Karstens, U., Minejima, C., and Mukai, H.: The CO_2 release and Oxygen uptake from Fossil Fuel Emission Estimate (COFFEE) dataset: Effects from varying oxidative ratios, in preparation, 2010.

Stephens, B. B.: Field-based Atmospheric Oxygen Measurements and the Ocean Carbon Cycle, PhD Thesis, Scripps Institution

of Oceanography, University of California, San Diego, 222 pp., 1999.

Stephens, B. B., Bakwin, P. S., Tans, P. P., Teclaw, R. M., and Baumann, D. D.: Application of a differential fuel-cell analyzer for measuring atmospheric oxygen variations, J. Atmos. Ocean. Tech., 24, 82–94, doi:10.1175/JTECH1959.1, 2007.

Stephens, B. B., Keeling, R. F., Heimann, M., Six, K. D., Murnane, R., and Caldeira, K.: Testing global ocean carbon cycle models using measurements of atmospheric O_2 and CO_2 concentration, Global Biogeochem. Cy., 12, 213–230, doi:10.1029/97GB03500, 1998.

Stephens, B. B., Keeling, R. F., and Paplawsky, W. J.: Shipboard measurements of atmospheric oxygen using a vacuum-ultraviolet absorption technique, Tellus B, 55, 857–878, doi:10.1046/j.1435-6935.2003.00075.x, 2003.

Sturm, P., Leuenberger, M., Sirignano, C., Neubert, R. E. M., Meijer, H. A. J., Langenfelds, R., Brand, W. A., and Tohjima, Y.: Permeation of atmospheric gases through polymer O-rings used in flasks for air sampling, J. Geophys. Res.-Atmos., 109, D04309, doi:10.1029/2003JD004073, 2004.

Thompson, R. L., Manning, A. C., Gloor, E., Schultz, U., Seifert, T., Hänsel, F., Jordan, A., and Heimann, M.: In-situ measurements of oxygen, carbon monoxide and greenhouse gases from Ochsenkopf tall tower in Germany, Atmos. Meas. Tech., 2, 573–591, doi:10.5194/amt-2-573-2009, 2009.

Thompson, R. L., Manning, A. C., Lowe, D. C., and Weatherburn, D. C.: A ship-based methodology for high precision atmospheric oxygen measurements and its application in the Southern Ocean region, Tellus B, 59, 643–653, doi:10.1111/j.1600-0889.2007.00292.x, 2007.

Tohjima, Y.: Method for measuring changes in the atmospheric O_2/N_2 ratio by a gas chromatograph equipped with a thermal conductivity detector, J. Geophys. Res.-Atmos., 105, 14575–14584, doi:10.1029/2000JD900057, 2000.

Tohjima, Y., Mukai, H., Nojiri, Y., Yamagishi, H., and Machida, T.: Atmospheric O_2/N_2 measurements at two Japanese sites: estimation of global oceanic and land biotic carbon sinks and analysis of the variations in atmospheric potential oxygen (APO), Tellus B, 60, 213–225, doi:10.1111/j.1600-0889.2007.00334.x, 2008.

Uglietti, C.: Understanding the Carbon Cycle through Atmospheric Carbon Dioxide and Oxygen Observations, PhD Thesis, Climate and Environmental Physics, Physics Institute, University of Bern, Bern, Switzerland, 159 pp., 2009.

van der Laan, S., Neubert, R. E. M., Karstens, U., van der Laan-Luijkx, I. T., and Meijer, H. A. J.: Fossil fuel based CO_2 emissions in the Netherlands based on ambient measurements and an improved [222]Radon flux method, Tellus B, 62(5), 389–402, doi:10.1111/j.1600-0889.2010.00493.x, 2010.

van der Laan, S., Neubert, R. E. M., and Meijer, H. A. J.: A single gas chromatograph for accurate atmospheric mixing ratio measurements of CO_2, CH_4, N_2O, SF_6 and CO, Atmos. Meas. Tech., 2, 549–559, doi:10.5194/amt-2-549-2009, 2009a.

van der Laan, S., Neubert, R. E. M., and Meijer, H. A. J.: Methane and nitrous oxide emissions in The Netherlands: ambient measurements support the national inventories, Atmos. Chem. Phys., 9, 9369–9379, doi:10.5194/acp-9-9369-2009, 2009b.

van der Laan-Luijkx, I. T.: Atmospheric oxygen and the global carbon cycle. Observations from the new F3 North Sea platform monitoring station and 6 additional locations in Europe and

Siberia, PhD Thesis, Centre for Isotope Research, University of Groningen, Groningen, the Netherlands, 191 pp., 2010.

van der Laan-Luijkx, I. T., Neubert, R. E. M., van der Laan, S., and Meijer, H. A. J.: Continuous measurements of atmospheric oxygen and carbon dioxide on a North Sea gas platform, Atmos. Meas. Tech., 3, 113–125, doi:10.5194/amt-3-113-2010, 2010.

Watson, A. J., Schuster, U., Bakker, D. C. E., Bates, N. R., Corbiere, A., Gonzalez-Davila, M., Friedrich, T., Hauck, J., Heinze, C., Johannessen, T., Kortzinger, A., Metzl, N., Olafsson, J., Olsen, A., Oschlies, A., Padin, X. A., Pfeil, B., Santana-Casiano, J. M., Steinhoff, T., Telszewski, M., Rios, A. F., Wallace, D. W. R., and Wanninkhof, R.: tracking the Variable North Atlantic Sink for Atmospheric CO_2, Science, 326, 1391–1393, doi:10.1126/science.1177394, 2009.

WMO: Report of the 14th WMO/IAEA Meeting of Experts on Carbon Dioxide Concentration and Related Tracers Measurement Techniques, Helsinki, Finland, 10–13 September 2007, World Meteorological Organization, Geneva, Switzerland, 2009.

Worthy, D. E. J., Platt, A., Kessler, R., Ernst, M., and Racki, S.: Measurement Procedures and Data Quality, Canadian Baseline Program; Summary of progress to 2002, Meteorological Service of Canada, 97–120, 2003.